ACS Macro Letters

Letter

pubs.acs.org/macroletters

Formation of a Rigid Amorphous Fraction in Poly(3-(2′-ethyl)hexylthiophene)

Bryan S. Beckingham,[†] Victor Ho,[†,‡] and Rachel A. Segalman*[,†,‡]

[†]Materials Science Division, Lawrence Berkeley National Laboratory, Berkeley, California 94720, United States

[‡]Department of Chemical and Biomolecular Engineering, University of California, Berkeley, California 94720, United States

Supporting Information

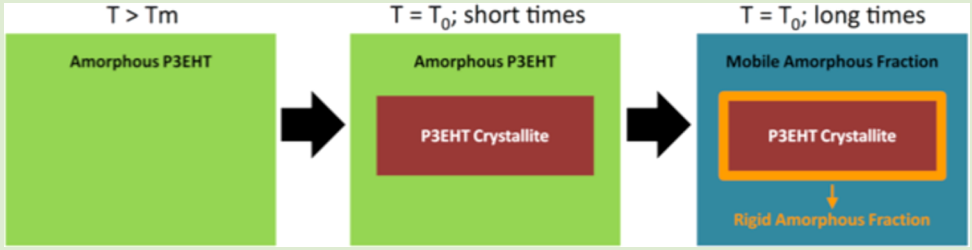

ABSTRACT: Herein, we detail the formation of a rigid amorphous fraction in poly(3-(2′-ethyl)hexylthiophene) (P3EHT) at high relative crystallinity, yielding a more complete picture of the solid-state structure. In the differential scanning calorimetry (DSC) heating scans of isothermally crystallized P3EHT a distinct endothermic peak appears slightly above the crystallization temperature. This previously undescribed endothermic feature of P3EHT's thermal behavior is observed consistently ∼20 °C above the crystallization temperature—shifting to higher temperatures with increasing crystallization temperature—and increases in magnitude with both time and crystallization temperature. Here, we determine the origins of this endothermic peak with DSC and temperature-modulated DSC (TMDSC). TMDSC reveals that the annealing peak observed in the total heat flow (THF)—heat flow equivalent to that of conventional DSC—is a consequence of an enthalpic relaxation observable as an endothermic peak in the nonreversible heat flow (NHF) and a glass transition evident as a step increase in the reversible heat flow (RHF). In conjunction with conventional DSC observations, these results indicate that the observed annealing peak is a consequence of the formation of distinct amorphous regions—a mobile amorphous fraction (MAF) and a rigid amorphous fraction (RAF)—during the isothermal crystallization process and not the melting of a distinct crystallite population or melt recrystallization.

In P3HT, and conjugated polymers in general, it is well-known that due to the intertwined nature of charge transport and the $\pi-\pi$ interactions between polymer chains within crystallites—as well as the molecular structure at crystallite boundaries—both the crystalline quality and overall polymer crystalline texture, or crystalline morphology, are of utmost importance to the resultant electrical properties. However, as P3HT forms a semicrystalline film upon solution-casting—the standard technique used in fabrication of such electronic devices—it has, in general, not been possible to control the nucleation and growth of the crystallites independent of the deposition conditions as the proximity of the melting transition to its thermal degradation preempts thermal treatments as a viable approach.[1] The fast crystallization kinetics and proximity of the melting and degradation temperatures of P3HT have hindered efforts to obtain precise control over the crystallite morphology via thermal processing and, perhaps more importantly, a rigorous understanding of its thermal behavior. This obstacle has been previously overcome by significantly depressing the thermal transitions through substitution of the hexyl side chain with a branched side chain.[2] Namely, while the straight side-chain variant poly(3-hexylthiophene) (P3HT) displays a melting transition over 200 °C, the branched analogue poly(3-(2′-ethyl)hexylthiophene) (P3EHT) exhibits a melting transition at more experimentally convenient temperature (T_m < 100 °C) and well below its thermal degradation. Thus, by facilitating thermal treatments to examine the fundamentals of crystallization in these materials, P3EHT is an ideal model polymer for examining the structure−property relationships in both homopolymers and block copolymers where manipulation of the morphology through thermal processing is imperative.[3−6]

Several studies have already endeavored to utilize the reduced melting transition of P3EHT to examine structure−property relationships in P3EHT.[2−5,7] Bourdouris and co-workers exploited the depressed melting temperature and slow crystallization kinetics of P3EHT to correlate the relative degree of crystallinity with the optoelectronic properties through UV−visible spectroscopy and field-effect transistor hole mobility measurements.[3] Additionally, while in P3HT-containing block copolymers microphase separation is precluded by crystallization of the P3HT, the full span of

Received: April 30, 2014
Accepted: June 28, 2014
Published: July 2, 2014

typical block copolymer morphologies is achievable using P3EHT, facilitating the formation of hierarchical structures via both microphase separation and crystallization.[7] While the propensity of P3EHT to form microphase-separated structures facilitates study of these hierarchal morphologies—i.e., P3EHT crystallite orientation in both confined geometries and the matrix—and how these structures affect material properties, fundamental questions remain as to the thermal behavior of the P3EHT homopolymer itself.

Importantly, upon examining, via differential scanning calorimetry (DSC), endotherms taken upon heating after isothermal crystallization of P3EHT, a distinct endothermic peak is observed ∼20 °C above the isothermal crystallization temperature. The appearance of this peak, typically referred to as an "annealing peak", just above the annealing temperature (here the isothermal crystallization temperature) is a common feature in semicrystalline polymers—such as polypropylene,[8,9] *cis*-1,4-polybutadiene,[10] poly(ethylene terepthalate),[11,12] poly(ether ether ketone),[13] polycarbonate,[8,14] and poly(3-hydroxy butyrate)[8] among others—and can typically be attributed to one of three mechanisms, namely, melt recrystallization, the presence of multiple distinct crystallite populations (in conjunction with the higher-temperature endothermic peaks discussed elsewhere[15]), or a physical aging (or relaxation) phenomenon originally discussed by Menczel and Wunderlich.[11] Understanding the phenomena behind this endothermic feature in the thermal behavior of P3EHT is vital to understanding the structural arrangement in the solid state—and thereby understanding how thermal manipulations of the structure are affecting optoelectronic properties—as this annealing peak signifies either the formation of or reorganization of the crystallite populations (melt recrystallization or multiple crystallite populations) or the state of the intercrystallite amorphous regions. In the case of melt recrystallization, the melting endotherm is attributed to the melting of a crystallite population formed during the preceding crystallization process. Upon heating, these crystallites are continually melted and recrystallized into progressively thicker, and/or more perfect, crystallites resulting in the presence of multiple, typically two, endothermic peaks: one from the initial crystallites that do not undergo recrystallization and a second higher melting endotherm resulting from the final melting of the thicker or more perfect crystallites.[16−18] Alternatively, the existence of multiple crystallite populations would attribute the observed endothermic peaks to the presence of multiple distinct crystallite populations formed during the initial crystallization process. Lastly, the physical aging model, as discussed here, corresponds to the formation of two distinct amorphous regions between crystallites, a central amorphous phase that is inherently more mobile, the so-called "mobile amorphous fraction" or MAF, and a more rigid amorphous phase around the crystallite−amorphous interfaces termed the "rigid amorphous fraction" or RAF. As the amorphous and crystalline phases are most often coupled due to the presence of tie chains and imperfect crystal fold surfaces, an intermediate phase of increased rigidity—resulting from being constrained at the crystal surface—between the crystallites and fully amorphous region (the central MAF region) has been recognized for many semicrystalline polymers.[8−14] The RAF region is typically characterized by an increased glass transition temperature and decreased density compared to the MAF, while it retains an identical chemical nature.[8−14]

Here, we examine the heretofore, to our knowledge, unexplained presence of the annealing peak observed after the isothermal crystallization of P3EHT to determine its origin and thereby a more informed depiction of the nanostructure. While we focus on P3EHT due to its accessible melting temperature, well below that of degradation, we note that similar endothermic peaks have been reported after isothermal crystallization of both poly(3-hexylthiophene)[19] and poly(3-dodecylthiophene)[20] such that this phenomenon may prove to be a more general feature of poly(alkylthiophenes). To this end, three P3EHTs (denoted P3EHT-X, where X is the Mn in kg/mol obtained from polystyrene-calibrated GPC) were synthesized via Grignard metathesis polymerization, characterized via gel permeation chromatography (GPC) (obtained molecular characteristics and GPC spectra are provided in the Supporting Information Table S-1 and Figure S-1, respectively) and the behavior of the observed low-temperature endothermic peak was systematically examined by DSC and TMDSC.

Prior to all scans, specimens were annealed above the melting temperature (at 130 °C) to remove the effects of prior thermal history. Samples were then quenched (∼32 °C/min) to a desired crystallization temperature (T_0) and held isothermally during crystallization. Conventional DSC was utilized to examine how the annealing peak varied with crystallization time and crystallization temperature. Endotherms of P3EHT-8, P3EHT-13, and P3EHT-23 taken upon heating at a rate of 10 °C/min after isothermal crystallization at 25 °C for various crystallization times, 15−300 min, are shown in Figure 1a−c, respectively. Similar experiments were completed with varied isothermal crystallization temperatures (T_0)—35, 40, 45, 50, and 55 °C—and the long-time melting endotherms obtained from these experiments are shown in Figure 2a, b, and c, for P3EHT-8, P3EHT-13, and P3EHT-23, respectively; the endotherms for the full range of crystallization time are provided in the Supporting Information (Figures S2−S4).

This report focuses on the behavior and origin of the lowest-temperature peak that is observed slightly above T_0—located at ∼45 °C in Figure 1, hereafter denoted T_A. The behavior and cause of the two higher-temperature endothermic peaks will be discussed in detail in a subsequent work.[15] It is clear from Figure 1 that the formation of the annealing peak is slow, as it is not observed, for example, in the case of P3EHT-8 in crystallization experiments under 140 min. Additionally, T_A shifts steadily to higher temperature with increasing crystallization temperature—consistently 20 ± 1 °C above T_0, as determined by a least-squares minimization—as observed qualitatively in Figure 2 and shown quantitatively in Figure 3 for P3EHT-23. These aspects of T_A's behavior—appearing at long crystallization times and regularly 20 °C above T_0—are both characteristics consistent with the formation of a rigid amorphous fraction.

To definitively identify the origin of T_A, further insight into its behavior was obtained from temperature-modulated differential scanning calorimetry (TMDSC). TMDSC is a useful extension of more traditional DSC in which a small sinusoidal oscillation or modulation is superimposed onto the conventional linear heating rate. This seemingly small addition is powerful in that it allows for measurement of the sample's heat capacity which in turn facilitates the separation of the total heat flow (THF), analogous to conventional DSC data, into the so-called reversible and nonreversible components of the heat flow or the RHF and NHF, respectively. It is important to note that the designation of reversible and nonreversible does not

dx.doi.org/10.1021/mz500262d | ACS Macro Lett. 2014, 3, 684−688

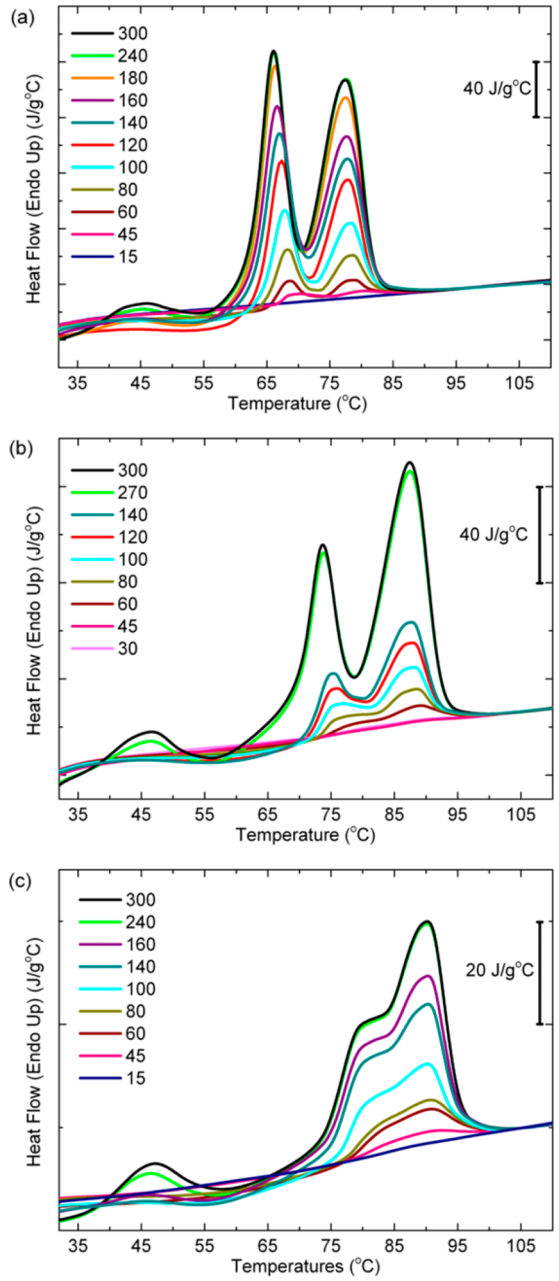

Figure 1. DSC endotherms of (a) P3EHT-8, (b) P3EHT-13, and (c) P3EHT-23 taken upon heating following isothermal crystallization for various times (in minutes as noted in legends) upon quenching from 130 to 25 °C.

indicate the reversibility of the observed signal but is derived from the fact that a material's true heat capacity is reversible and that the RHF provides information pertaining to heat-capacity related heat flow, whereas the NHF is related to kinetics-related heat flow. Therefore, melting-related heat flow is observed in both the RHF and NHF, but crystallization and enthalpic relaxation/recovery are only detected in the NHF. This allows for separation of phenomena such as crystallization or recrystallization from glass transitions and most melting.

As can be seen in Figure 4 (for the full endotherms, see the Supporting Information Figure S-5) the annealing peak observed in traditional DSC is observed in the total heat flow and separated into an endothermic peak in the nonreversible heat flow and a glass transition step in the reversible heat flow.

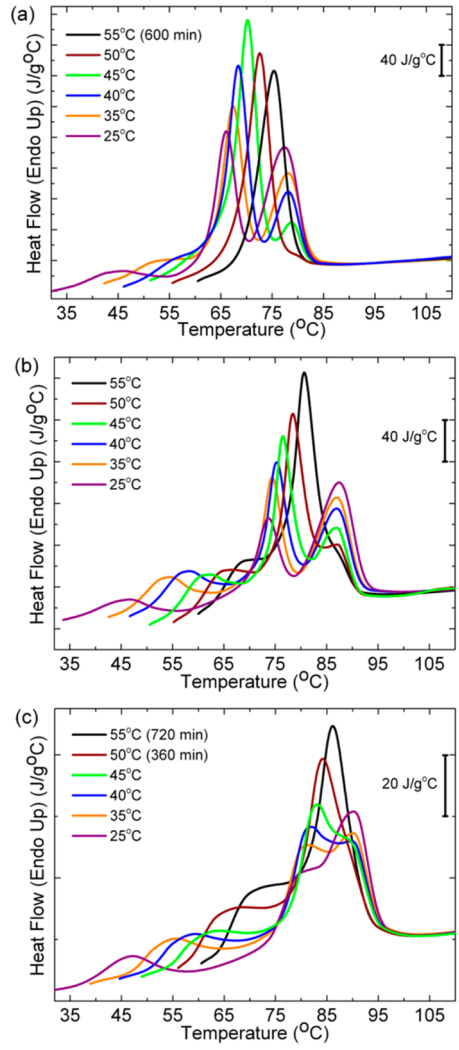

Figure 2. DSC endotherms of (a) P3EHT-8, (b) P3EHT-13, and (c) P3EHT-23 taken upon heating following isothermal crystallization at 25, 35, 40, 45, 50, and 55 °C for 300 min, unless noted, after quenching from 130 °C.

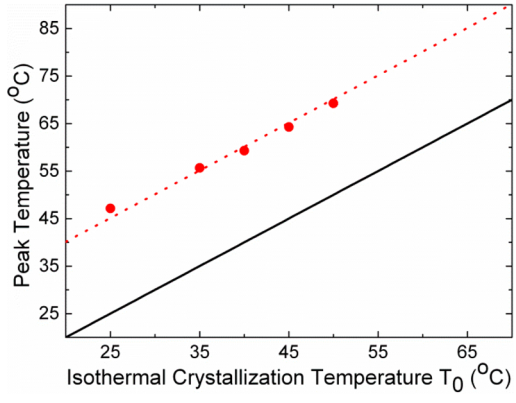

Figure 3. Peak temperature (red circle) of the annealing peak, T_A, observed for P3EHT-23 plotted as a function of the isothermal crystallization temperature, T_0. Points obtained using a Gaussian fit to the long-time isothermal crystallization data shown in Figure 2c. Black solid line (−) represents $T_A = T_0$, and the red dotted line (---) represents $T_A = T_0 + b$, where b (20.1) is determined by a least-squares minimization.

dx.doi.org/10.1021/mz500262d | ACS Macro Lett. 2014, 3, 684−688

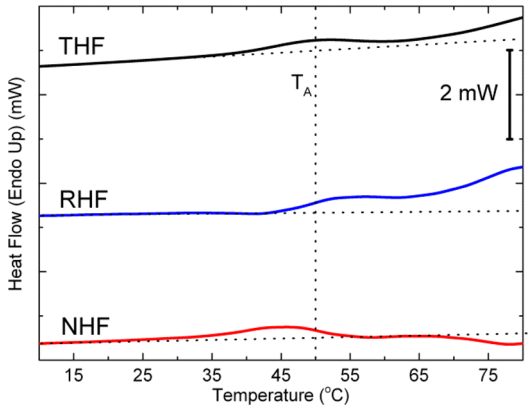

Figure 4. Temperature-modulated differential scanning calorimetry of P3EHT-23, where the black line represents the total heat flow, the blue line represents the reversible heat flow, and the red line represents the nonreversible heat flow. Horizontal dotted lines represent baseline fits to the endotherms, whereas the vertical dotted line denotes the position of T_A in the total heat flow. A heating rate of 10 °C/min was used with a temperature-modulation amplitude of 0.5 °C and modulation period of 1 min.

While the glass transition in the RHF corresponds to the devitrification of the RAF, the endothermic peak observed in the NHF can be attributed to an enthalpic relaxation of the rigid amorphous fraction as has been identified via TMDSC for various other semicrystalline polymers.[21−23]

While the presence of a glass transition and enthalpic relaxation is consistent with the presence of a rigid amorphous fraction, the obtained TMDSC data must also be discussed within the context of the melt recrystallization and multiple crystallite population models to determine their feasibility as causes of T_A. First, in the case of melt recrystallization an endothermic peak in the RHF and exothermic peak in the NHF would be observed simultaneously due to the ongoing melting and crystallization processes, respectively. As an endothermic and not exothermic peak is observed in the NHF, the possibility of T_A resulting from a melt-recrystallization process can be excluded. For T_A resulting from the presence of a unique crystallite population, only a peak in the RHF—due to crystallite melting—would be expected, whereas in the obtained TMDSC data a step increase in the RHF and an endothermic peak in the NHF are observed. We thereby find that the obtained TMDSC data are consistent with the formation of a rigid amorphous fraction at long times (high relative crystallinity) during the isothermal crystallization of P3EHT. The observed peak in DSC is thus due to the presence of a rigid amorphous fraction undergoing a simultaneous devitrification and enthalpic relaxation.

The endothermic annealing peak observed at long times upon heating isothermally crystallized P3EHT is found, via DSC, to shift linearly to higher peak temperatures with increasing isothermal crystallization temperature. This shift in peak temperature and its appearance at long times is consistent with the formation of a rigid amorphous fraction or RAF. The presence of RAF formation in P3EHT is confirmed using TMDSC where the endothermic peak observed in conventional DSC is resolved into a glass transition step apparent in the reversible heat flow and an endothermic peak in the nonreversible heat flow. These findings are both consistent with the formation of RAF and inconsistent with alternative origins of this peak, namely, melt recrystallization and the presence of a distinct crystallite population, thereby confirming the existence of RAF in P3EHT. The formation of this rigid amorphous fraction has, to our knowledge, not been previously discussed in P3EHT. However, Pal and Nandi have attributed, in part, the low Avrami exponents obtained for P3EHT and P3OT to the "soft impingement" of the growing crystallites by a rigid amorphous fraction as described by Cheng and Wunderlich.[24,25] The presence of this RAF is possibly of great importance not only to P3EHT's properties but also to those of other polyalkylthiophenes, namely, P3HT, in general. As these materials find significant use as active layer optoelectronic materials the occurrence, or deliberate manipulation, of a rigid amorphous fraction could have profound effects on their behavior optoelectronically, effects we are currently probing. Overall, this enhanced understanding of P3EHT's solid-state nanostructure can aid in the formulation of improved processing protocols for this class of materials, potentially leading to the improvement of organic electronic devices.

■ ASSOCIATED CONTENT

Supporting Information

Detailed synthetic and experimental techniques and additional DSC and TMDSC data. This material is available free of charge via the Internet at http://pubs.acs.org.

■ AUTHOR INFORMATION

Corresponding Author

*E-mail: segalman@engineering.ucsb.edu.

Notes

The authors declare no competing financial interest.

■ ACKNOWLEDGMENTS

The authors graciously thank Jesus Guardado for his aid in performing the TMDSC experiments and the Stanford Nano Center for use of the TA Q2000 TMDSC. BSB gratefully acknowledges support from the U.S. Department of Energy (DOE), Office of Science, Basic Energy Sciences (BES) under Award #DE-AC02-05CH11231. V.H. and R.A.S. gratefully acknowledge support from the National Science Foundation, DMR-1206296.

■ REFERENCES

(1) Kuila, B. K.; Nandi, A. K. *J. Phys. Chem. B* **2006**, *110*, 1621−1631.
(2) Ho, V.; Boudouris, B. W.; Segalman, R. A. *Macromolecules* **2010**, *43* (19), 7895−7899.
(3) Boudouris, B. W.; Ho, V.; Jimison, L. H.; Toney, M. F.; Salleo, A.; Segalman, R. A. *Macromolecules* **2011**, *44* (17), 6653−6658.
(4) Ho, V.; Boudouris, B. W.; McCulloch, B. L.; Shuttle, C. G.; Burkhardt, M.; Chabinyc, M. L.; Segalman, R. A. *J. Am. Chem. Soc.* **2011**, *133* (24), 9270−9273.
(5) Patel, S. N.; Javier, A. E.; Beers, K. M.; Pople, J. A.; Ho, V.; Segalman, R. A.; Balsara, N. P. *Nano Lett.* **2012**, *12* (9), 4901−4906.
(6) Lin, S. H.; Wu, S. J.; Ho, C. C.; Su, W. F. *Macromolecules* **2013**, *46* (7), 2725−2732.
(7) McCulloch, B.; Ho, V.; Hoarfrost, M.; Stanley, C.; Do, C.; Heller, W. T.; Segalman, R. A. *Macromolecules* **2013**, *46* (5), 1899−1907.
(8) Schick, C.; Wurm, A.; Mohammed, A. *Thermochim. Acta* **2002**, *392*−*393*, 202−313.
(9) Grebowicz, J.; Lai, S. F.; Wunderlich, B. *J. Polym. Sci., Polym. Symp.* **1984**, *71*, 19−37.
(10) Di Lorenzo, M. L. *Polymer* **2009**, *50*, 578−584.
(11) Menczel, J.; Wunderlich, B. *J. Polym. Sci., Poly. Lett.* **1985**, *19*, 261−264.

(12) Lin, J.; Shenogin, S.; Nazarenko, S. *Polymer* **2002**, *43*, 4733−4743.
(13) Cheng, S. Z. D.; Pan, R.; Wunderlich, B. *Makromol. Chem.* **1988**, *189*, 2443−2458.
(14) Schick, C.; Wurm, A.; Merzylyakov, M.; Minakov, A.; Marand, H. J. *Therm. Anal. Calorim.* **2001**, *64*, 549−555.
(15) Beckingham, B. S.; Ho, V.; Segalman, R. A. in Preparation.
(16) Boon, J.; Challa, G.; Van Krevelen, D. W. *J. Polym. Sci., Part A: Gen. Pap.* **1968**, *2*, 1791.
(17) Lemstra, P. J.; Kooistra, T.; Challa, G. *J. Polym. Sci. Polym. Phys. Ed.* **1974**, *12*, 1565.
(18) Blundell, D. J. *Polymer* **1987**, *28*, 2248.
(19) Zhao, Y.; Yuan, G.; Roche, P.; Leclerc, M. *Polymer* **1995**, *36*, 2211−2214.
(20) Park, K. C.; Levon, K. *Macromolecules* **1997**, *30*, 3175−3183.
(21) Bai, H.; Luo, F.; Zhou, T.; Deng, H.; Wang, K.; Fu, Q. *Polymer* **2011**, *52*, 2351−2360.
(22) Bonnet, M.; Rogausch, K.-D.; Peterman, J. *Colloid Polym. Sci.* **1999**, *277*, 513−518.
(23) Liu, T. *Eur. Polym. J.* **2003**, *39*, 1311−1317.
(24) Pal, S.; Nandi, A. K. *Polymer* **2005**, *46*, 8321−8330.
(25) Cheng, S. Z. D.; Wunderlich, B. *Macromolecules* **1988**, *21*, 3327−3328.